Available online at www.sciencedirect.com
ScienceDirect
International Journal of Pharmaceutics 353 (2008) 205–222
INTERNATIONAL JOURNAL OF PHARMACEUTICS
www.elsevier.com/locate/ijpharm

Dexamethasone transport and ocular delivery from poly(hydroxyethyl methacrylate) gels

Jinah Kim, Anuj Chauhan *

Department of Chemical Engineering, University of Florida, Gainesville, FL 32611, United States

Received 5 July 2007; received in revised form 15 November 2007; accepted 20 November 2007
Available online 8 December 2007

Abstract

We explore ocular delivery of dexamethasone (DX) via poly(hydroxyethyl methacrylate) (PHEMA) contact lenses, which are known to have a much higher bioavailability in comparison to eye drops. Three derivatives of dexamethasone (dexamethasone 21-disodium phosphate (DXP), dexamethasone, and dexamethasone 21-acetate (DXA)) are explored. These drugs are loaded in the gels by soaking in aqueous or ethanol solutions, and also by direct addition of the drug to the polymerizing mixture. Dynamic drug concentrations in the aqueous phase are monitored both in loading and release experiments. The data is utilized to determine the partition coefficients and the mean diffusivity, which includes contributions from both bulk and surface diffusion. Finally we utilize the transport model to predict the bioavailability of the three forms of dexamethasone for drug delivery via contact lenses. The transport of each of the drug is diffusion limited with diffusivities of 1.08×10^{-11} and 1.16×10^{-11} m^2/s for DX and DXA, respectively. The diffusivities of DXP depend on concentration and on ionic strength, and are much smaller than those for DX and DXP. The bioavailability for delivery of these drugs via contact lenses is much higher than that for drops, and the bioavailability is the highest for DXA.

Keywords: Dexamethasone; Dexamethasone acetate; Dexamethasone phosphate; Contact lenses; HEMA; Diffusivity; Crosslinking; Charged drugs; Model; Salt effect

1. Introduction

In the last few decades, a number of novel approaches have been developed for controlled drug delivery of ophthalmic drugs. However, most treatments of ocular disease are still based on topical application of eye drops to the surface of the eye (Ogura, 2001). After application of an eye drop, the drug solution mixes with tear fluid, and then within about 5 min, a majority of drug is eliminated by tear drainage and conjunctival uptake. Due to the short residence time, only about 1–5% of the applied drug penetrates the cornea and reaches the intraocular tissues. To maintain therapeutic levels of drug concentration, frequent instillation of drops with large drug loadings are required, which is inconvenient for patients. Moreover, the drug that gets absorbed in conjunctiva or in the nasal cavity eventually reaches other organs through the blood circulation leading to side effects (Ahmed and Patton, 1985, 1987). To overcome the drawbacks of eye drops, several ophthalmic drug delivery systems have been proposed such as suspension of nanoparticles, nanocapsules, liposomes and niosomes, ocular inserts like collagen shields and Ocusert®, and therapeutic contact lenses. Among theses, contact lenses have been widely studied due to the high degree of comfort and biocompatibility. On instillation of medicated contact lens in the eye, drug diffuses through the lens matrix into the thin tear film named post-lens tear film (POLTF) trapped between the lens and the cornea, and the drug has a residence time about 30 min in the eye (Mcnamara et al., 1999; Creech et al., 2001). An increase in the residence time leads to a significant increase in the bioavailability. Both mathematical models and clinical data suggest that the bioavailability for ophthalmic drug delivery can be as large as 50%, which is an order of magnitude larger than that for drops (Li and Chauhan, 2006).

Most of the studies on drug delivery by contact lenses focused on soaking the lens in concentrated drug solution to load the drug, followed by *in vitro* or *in vivo* release studies (Hillman, 1974; Ramer and Gasset, 1974; Ruben and Watkins, 1975;

* Corresponding author. Tel.: +1 352 392 2592; fax: +1 352 392 9513.
E-mail address: Chauhan@che.ufl.edu (A. Chauhan).

0378-5173/$ – see front matter © 2007 Elsevier B.V. All rights reserved.
doi:10.1016/j.ijpharm.2007.11.049

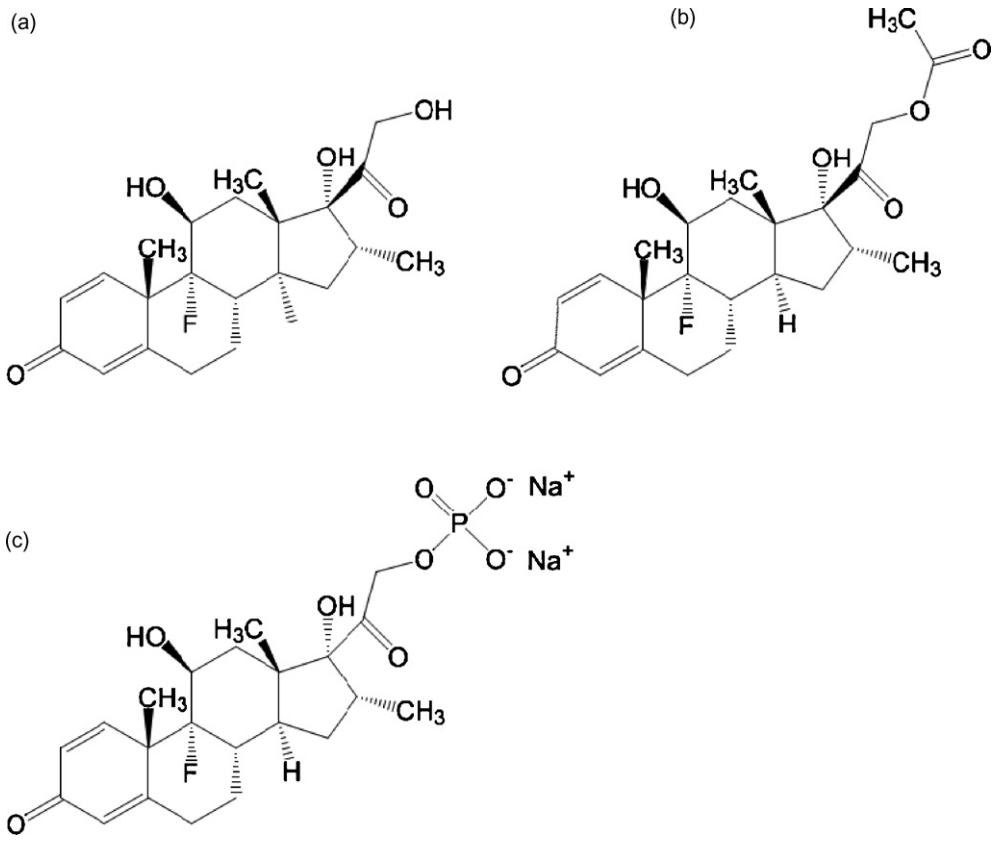

Fig. 1. Molecular structures of model drugs: (a) DX; (b) DXA; (c) DXP.

Arthur et al., 1983; Rosenwald, 1984; Wilson and Shields, 1989; Fristrom, 1996; Schultz et al., 1998; Schultz and Mint, 2002). In some cases, the loading capacity of the soaked contact lenses is inadequate. The loading capacity can be increased by a number of approaches such as by designing a molecularly imprinted soft contact lens. It has been demonstrated both by *in vivo* and *in vitro* studies that soft contact lenses fabricated by the molecular imprinting method have a drug loading capacity 2- to 3-fold greater than that of the contact lenses made by a conventional method (Hiratani and Alvarez-Lorenzo, 2004; Hiratani et al., 2005). Another commonly used method of entrapping drugs in gels is direct addition of drug in the polymerizing medium (Ende and Peppas, 1997; Colombo et al., 1999; Ward and Peppas, 2001).

The drug of interest for this study is dexamethasone (DX). Dexamethasone is a glucocorticoid steroid, which is similar to the natural steroid hormone made by the adrenal glands in the body. It relieves eye inflammation and swelling, heat, redness, and pain caused by chemicals, infection, and/or severe allergies. It is also used to treat persistent macular oedema in retina, which is a major cause of visual disabilities and blindness among individuals with diabetes (Clark and Yorio, 2003). Prolonged systemic administration of steroid can cause serious side effects such as diabetes, hemorrhagic ulcers, skin atrophy, myopathies, osteoporosis and psychosis (Melby, 1974). Furthermore, it has been reported that continuous application of eye drops of 0.1% dexamethasone for extended periods of time (varying from 3 weeks to 1 year) can cause glaucoma accompanied by optic nerve damage, defects in visual acuity and fields of vision, and posterior subcapsular cataract formation and thinning of the cornea or sclera (Schwartz, 1966; Urban and Cotlier, 1986). Controlled drug delivery of dexamethasone to the eye through daily wear contact lens is expected to be safer than delivery via drops because of reduction in the amount of drug that reaches other body tissues through systemic circulation (Li and Chauhan, 2006). Several forms of dexamethasone with significantly different aqueous solubilities have been utilized in ocular studies including dexamethasone 21-disodium phosphate (DXP), dexamethasone, and dexamethasone 21-acetate (DXA) (arranged in the order of increasing partition coefficients measured in octanol-phosphate buffer solution) (Einmahl et al., 1999; Civiale et al., 2004). Molecular structures of these three dexamethasone derivatives are shown in Fig. 1. Dexamethasone and dexamethasone 21-acetate are hydrophobic drugs while dexamethasone 21-disodium phosphate is ionic and thus freely water soluble. Civiale et al. screened the ocular permeability of dexamethasone derivatives through cell culture (*in vitro*) and excised rabbit cornea (*ex vivo*) and studied *in vivo* concentration of dexamethasone in rabbit aqueous humor as well. They reported that the permeability rates of dexamethasone derivates through cornea generally increase as octanol/water partitioning coefficients (log *P*) increase (Civiale et al., 2004). Weijtens et al. determined the dexamethasone concentration in aqueous humor, vitreous and serum after dexamethasone administration through various routes such as topical application of eye drop, subconjunctival injection, a peribulbar injection, and an oral

dose (Weijtens et al., 1997, 1998, 1999, 2000, 2002). They showed that the dexamethasone concentration in the aqueous humor is far lower for eye drops of 0.1% dexamethasone disodium phosphate compared to a subconjunctival injection even if an eye drop is instilled every 1.5 h. However the conjunctival injection is also not the optimal drug delivery vehicle because it needs to be applied daily to have sufficiently high dexamethasone concentrations in the aqueous humor. It is thus desirable to have other drug delivery vehicles that can deliver dexamethasone in a non-invasive manner, and yet achieve sufficiently high concentrations in aqueous humor.

The aim of this study was to investigate loading and release of different forms of dexamethasone in poly(hydroxyethyl methacrylate) (PHEMA) gels, which are a common contact lens material. Three different derivatives of dexamethasone, i.e., dexamethasone, dexamethasone 21-acetate, and dexamethasone 21-disodium phosphate were incorporated in the gel by soaking gels in drug solutions (soaking method) or by direct dissolution of the drug in the polymerizing mixture (direct entrapment method). The loaded drug was then released by soaking the drug-loaded gels in deionized (DI) water or PBS. Dynamic drug concentrations in the aqueous phase were monitored both in loading and release experiments. The equilibrium uptake in these experiments was utilized to determine the partition coefficients, and the dynamic data was fitted to a modified diffusion equation to determine the mean diffusivity, which includes contributions from both bulk and surface diffusion. Finally the transport model for the drugs was utilized to predict the bioavailability of the three forms of dexamethasone for drug delivery via PHEMA contact lenses.

2. Materials and methods

2.1. Materials

2-Hydroxyethyl methacrylate (HEMA, 97%) monomer, dexamethasone 21-acetate (≥99%), dexamethasone 21-disodium phosphate (≥99%), timolol maleate (≥98%), ethanol (≥99.5%), and Dulbecco's phosphate buffered saline (PBS) were purchased from Sigma–Aldrich Chemicals (St. Louis, MO); dexamethasone (DX, 98%) and ethylene glycol dimethacrylate (EGDMA) from Sigma–Aldrich Chemicals (Milwaukee, WI). Darocur® TPO was kindly provided by Ciba Specialty Chemicals (Tarrytown, NY). Nitrogen was bought from Praxair (Danbury, CT). All the other chemicals were of reagent grade. All the chemicals were used without further purification.

2.2. Methods

2.2.1. Synthesis of PHEMA gels

Poly(hydroxyethyl methacrylate) gels were synthesized by free radical solution or bulk polymerization of the monomer with photoinitiation. Briefly, 2.7 ml of monomer HEMA and 10 μl of EGDMA were mixed with 2 ml of deionized (DI) water. The solution was purged by bubbling nitrogen for 10 min. 6 μg of photoinitiator (Darocur® TPO) was added to the monomer mixture with stirring for 5 min and the resulting solution was immediately injected into a mold composed of two 5 mm thick glass plates separated by a plastic spacer. The spacer thickness was chosen to be either 0.1 or 0.2 mm. The mold was then placed on Ultraviolet transilluminiator UVB-10 (Ultra·Lum, Inc.) and the gel was cured by irradiating by UVB light (305 nm) for 40 min. The gel was cut in square shaped pieces (about 1.5 cm × 1.5 cm) and dried in air overnight for further use.

2.2.2. Drug loading

The drug was loaded into the gels either by directly dissolving the drug in the polymerizing mixture (direct entrapment) or by soaking the gel in an aqueous drug solution. Due to minimal solubility of DXA in water, it was loaded by direct entrapment or by soaking the gel in drug–ethanol solution. The drug concentrations in the loading solutions and the drug loading by direct entrapment were conducted under conditions that led to drug loadings comparable to those required for therapeutic applications. Before the soaking step, a square piece of PHEMA gel (about 1.5 cm × 1.5 cm) was boiled in 200 ml of DI water for 30 min to remove the unreacted monomer. Next the gel was soaked in 3 ml of drug solution. DXA was loaded by soaking in drug–ethanol solution for a period of 3 h. During the soaking in drug–ethanol solution, the dynamic concentration in the ethanol phase was not monitored. The total amount of drug loaded into the gel was estimated by determining the amount of ethanol uptake by the gel, and then multiplying it by the drug concentration in the ethanol solution. It was thus implicitly assumed that in view of the very high solubility of DXA in ethanol, absorption of drug on the PHEMA polymer can be neglected when the gel is soaked in ethanol. At the end of the loading stage the gel was taken out and dried in air overnight, and subsequently used for release experiments.

During soaking of gels in aqueous DX and DXP solutions, the dynamic drug concentration in the DI water (or PBS) was monitored by measuring the absorbance spectra of the solution over the wavelength range of 220–270 nm with a UV–VIS spectrophotometer (Thermospectronic Genesys 10 UV). The loading step was conducted till equilibrium was reached. The total amount of drug loaded into the gel was determined by finding the total amount of drug loss from the aqueous solution.

2.2.3. Drug release experiments

The drug release experiments were conducted by soaking the square shaped gels (about 1.5 cm × 1.5 cm) in 3 ml of DI water (or PBS) at room temperature. It is noted that the gels that were loaded with drug by soaking in aqueous solutions were directly transferred from the loading solution to the release solution, and so these were fully hydrated at the beginning of the release experiment. However, gels that had the drug loaded by direct entrapment or by soaking in drug–ethanol solution were dry at the beginning of the release experiment. The effect of this difference was shown to be minimal by comparing release profiles from dry and hydrated gels with the same drug loading (results not shown here). During the release experiments, the dynamic drug concentration in the DI water (or PBS) was monitored by measuring the absorbance spectra of the solution over the wavelength range of 220–270 nm. After equilibrium was reached, the

gels were transferred to fresh 3 ml solution (DI water or PBS) and the process was repeated. These two releases are refereed as the 1st and the 2nd release. In some cases even a 3rd release was performed.

2.2.4. Effect of gel thickness on loading and release of drug (DX, DXA, or DXP)

To determine whether the drug transport in gels is controlled by diffusion, the procedures described above were repeated with thin gels (0.1 mm thick). The drug loading and release procedures for the thin gels were identical to those described above except that the volume of solutions was reduced by a factor of 2 to ensure that the ratio of gel to fluid volume was kept the same.

2.2.5. Effect of ionic strength in release solution on loading and release of DXP

Since DXP is a charged molecule, its transport may be affected by the ionic strength. To investigate the effect of electrostatics on DXP transport, the loading and release experiments for DXP were conducted at several different ionic strengths. In these experiments the ionic strength was changed by adding NaCl to the PBS buffer. DXP loading and release experiments were carried with three different NaCl–DXP solution in PBS corresponding ionic strengths of 594, 1022, and 1202 mM. Also experiments were conducted in PBS that has an ionic strength of 173 mM.

2.2.6. Conversion of UV–vis absorbance to the corresponding concentration of drug

The absorbencies of solution in both the loading and the release steps arise mainly from the drug, but there is some additional absorbance due to small polymer chains that continue to diffuse out from the PHEMA gels. The absorbance spectra of HEMA and dexamethasone (DX, DXA, and DXP) partially overlap, and thus to distinguish between the absorbance from HEMA and the drug, the measured absorbance spectra was deconvoluted by expressing the measured absorbance as

$$\text{Abs} = \alpha \times \text{Drug} + \beta \times \text{Control} \tag{1}$$

where Abs is the measured absorbance spectra from 220 to 270 nm, Drug is the absorbance spectra of the drug in the same wavelength range at some arbitrary concentration, Control is the absorbance spectra of the solution in which PHEMA gel without any drug was soaked, and α and β are constants. These constants were obtained by finding best fit values minimizing the error between measured absorbance and calculated absorbance according to Eq. (1) using the function 'fminsearch' in MATLAB. The concentration of drug was finally obtained by multiplying α to the concentration corresponding to Drug. The above procedure assumes that the absorbencies of these components are simply additive and linear in concentration, and this was verified by conducting several experiments. Also the accuracy of the procedure described above was established by determining drug concentrations in solutions of known composition. The difference between the fitted and the measured absorbance spectra was typically less than 1%.

2.2.7. Determinations of critical micelle concentration (CMC) of DXP

Surface tension isotherm of DXP was measured at room temperature (about 23 °C) by creating a pendant drop, digitizing the shape and then fitting it to the Young-Laplace equation by using the Drop Shape Analysis System DSA100 (KRÜSS). A concentrated solution of the DXP (40 mg/ml) in PBS was prepared and then diluted successively to 0.021 mg/ml which is far below the expected CMC.

3. Results and discussion

3.1. DX loaded gel

3.1.1. DX loading (by soaking in aqueous solution) and release studies

3.1.1.1. Partition coefficient. The partition coefficient K is defined as the ratio of the drug concentration in the gel and the concentration in the aqueous phase at equilibrium. The values of partition coefficient can be obtained from both the loading and the release experiments. For the loading experiment the partition coefficient can be calculated by

$$K = \frac{C_{g,f}}{C_{w,f}} = \frac{V_w(C_{w,i} - C_{w,f})}{V_g C_{w,f}}, \tag{2}$$

where V_w and V_g are the volumes of the aqueous phase and the fully hydrated gel, respectively, and $C_{g,f}$, $C_{w,i}$ and $C_{w,f}$ are the equilibrium concentrations of the drug in the gel, and the initial and equilibrium concentrations in the aqueous phase, respectively, in the loading experiment. For the 1st release, the partition coefficient is given by

$$K = \frac{C_{g,f}}{C_{w,f}} = \frac{V_w(C_{w,i} - C_{w,f} - C_{r,f})}{V_g C_{r,f}} \tag{3}$$

where $C_{r,f}$ is the equilibrium concentration of the drug in the aqueous phase gel in the 1st release, and the other variables correspond to the values obtained from the loading phase for the same gel. Similar expressions can be written for the 2nd and the 3rd releases.

Table 1 shows the equilibrium concentrations in the water phase and corresponding partition coefficients. The partition coefficient of DX seems to be constant in the whole concentration range that was explored in these experiments. Moreover, the K values are similar for the loading, 1st release, and 2nd release. This suggests that the process of loading and release of DX is reversible and that K is not function of concentration in the explored concentration range. The K values for loading and release were 39.00 ± 3.14 and 37.00 ± 3.41, respectively and mean K was 38.00.

3.1.1.2. Dynamics of DX loading. A schematic of the geometry of the gel used in the drug loading and release experiments is shown in Fig. 2. The experimental data shown above demonstrates that the partition coefficient for dexamethasone is much larger than 1, which implies that a large fraction of the drug is bound to the PHEMA polymer. The binding of the drug to the

Table 1
DX concentration and partition coefficients (K) of DX in a soaking method

No.	$C_{w,f}$ (mg/ml)	$C_{w,i}$ (loading) (mg/ml)	M_0/M_g (release) (mg/g)	K
Loading				
1	0.014	0.026		37.54
2	0.015	0.026		35.61
3	0.020	0.038		41.65
4	0.027	0.051		37.50
5	0.028	0.051		40.72
6	0.033	0.058		43.38
7	0.033	0.058		43.00
8	0.035	0.064		39.82
9	0.043	0.077		35.83
10	0.045	0.077		34.90
1st release				
1	0.006		0.69	38.40
4	0.013		1.37	38.91
10	0.018		2.11	36.37
2nd release				
1	0.003		0.33	36.81
4	0.006		0.66	40.69
10	0.008		0.90	30.81

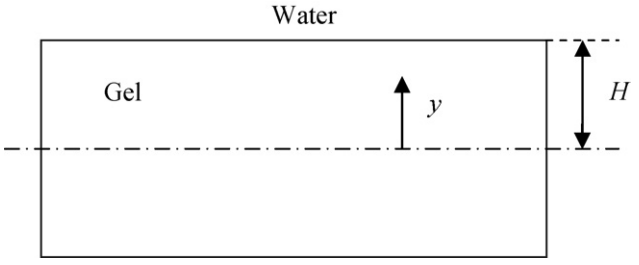

Fig. 2. The model geometry of the gel.

gel can be modeled as a Langmuir adsorption isotherm, which relates the adsorbed concentration of the drug on the gel (Γ) to the free concentration in the aqueous phase inside the gel (C) by the following equation

$$\Gamma = \frac{\Gamma_\infty C}{k + C} \tag{4}$$

where Γ_∞ is the surface concentration at the maximum packing on the surface and k is the ratio of the rate constants for desorption and adsorption of the drug on the HEMA surface. The mean concentration in the gel (C_g), which is essentially the sum of the bound concentration and the free concentration, is given by

$$C_g = \left(\frac{S}{V}\right)_{gel} \Gamma + fC \tag{5}$$

where $(S/V)_{gel}$ is the surface area per volume available for the drug to adsorb and f is the volume fraction of water in hydrated gel. The value of f for PHEMA gels was determined to be 0.42 from the swelling experiments. At equilibrium the free drug concentration in the gel is expected to equal to the concentration in the PBS, and thus the partition coefficients determined above are simply the ratio of the total drug and the free drug, i.e.,

$$K \equiv \frac{C_g}{C} = \frac{a}{k + C} + f \tag{6}$$

where $a \equiv (S/V)_{gel}\Gamma_\infty$. The values of K shown above are independent of C, which suggests that the value of k for DX adsorption on HEMA is much larger than 0.045 mg/ml which is the highest equilibrium concentration investigated in this study. Thus K is treated as independent of concentration in the model developed below. The transport of the drug in the hydrogel is expected to occur by a combination of bulk and surface diffusion, and thus it can be described by the modified diffusion equation, i.e.,

$$\frac{\partial(C_g)}{\partial t} = fD_f \frac{\partial^2 C}{\partial y^2} + D_s \left(\frac{P}{A}\right) \frac{\partial^2 \Gamma}{\partial y^2} \tag{7}$$

where D_f and D_s are the diffusivities of the drug in solution and on the surface, respectively, and P/A is the perimeter of the gel fibers per unit cross-sectional area, which can be approximated as S/V. Utilizing (5) and (6) in the above equation and noting the fact that K is independent of C gives

$$K\frac{\partial C}{\partial t} = (fD_f + D_s(K - f))\frac{\partial^2 C}{\partial y^2} = D\frac{\partial^2 C}{\partial y^2} \tag{8}$$

where $D \equiv (fD_f + D_s(K - f))$ is the effective diffusivity of drug in the gel. The above differential equation is subjected to the following boundary conditions

$$\left.\frac{\partial C}{\partial y}(t, y)\right|_{y=0} = 0, \tag{9a}$$

$$C(t, y = H) = C_w \tag{9b}$$

where H is the half thickness of the gel. The boundary condition (9a) arises due to symmetry at the center of the gel and the boundary condition (9b) assumes that the drug concentration in the water phase in the gel phase at the interface of gel and solution is the same as the concentration in the outer water phase.

From a mass balance of drug in the aqueous phase, we get

$$V_w \frac{dC_w}{dt} = -2A_g D \left.\frac{\partial C}{\partial y}\right|_{y=H} \tag{10}$$

where A_g is a cross-sectional area of the gel.

The initial conditions for the drug loading are

$$C_w(t = 0) = C_{w,i} \tag{11a}$$

$$C(t = 0, y) = 0 \tag{11b}$$

The above set of equations was solved by implicit finite difference method with 21 spatial nodes and a dimensionless time step ($D\Delta t/KH^2$) of 0.0025. The DX loading experiments were conducted with different initial concentrations and the dynamic drug concentration in the aqueous phase was measured. These data was fitted to the model described above and diffusivity of the drug in the gel was determined. The error between the experimental data and model prediction was defined as $\sqrt{\sum(C_w - C_{w,ex})^2}/\sum C_{w,ex}$, where C_w and $C_{w,ex}$ are the predicted concentration in the aqueous phase by model and the

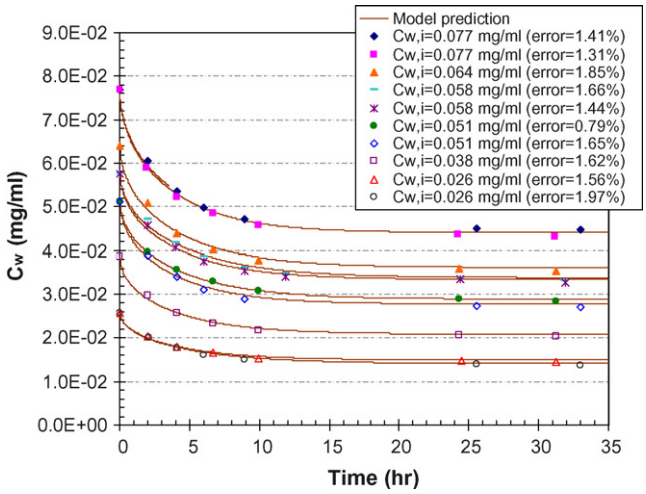

Fig. 3. Comparison of the model prediction and experimental data for DX loading into PHEMA gel soaked in drug solution. Initial drug concentration in the aqueous phase and rms errors are indicated. $K = 39.00 \pm 3.14$ and $D = 1.04 \times 10^{-11} \pm 5.85 \times 10^{-13}$ m^2/s ($n = 10$).

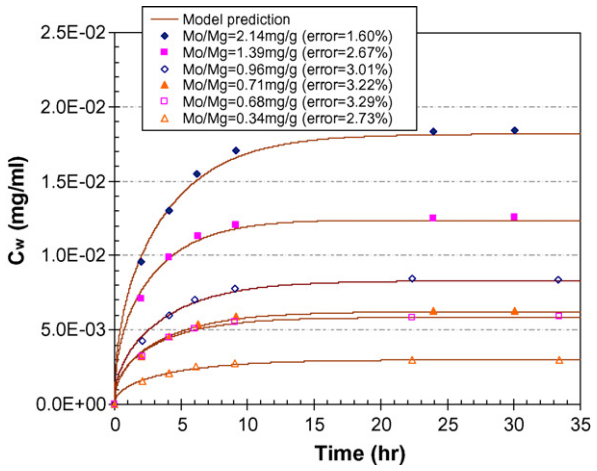

Fig. 4. Comparison of the model prediction and experimental data for DX release into fresh water from a PHEMA gels which have been soaked in drug solution. $K = 37.00 \pm 3.41$ and $D = 1.06 \times 10^{-11} \pm 1.48 \times 10^{-12}$ m^2/s ($n = 6$). Initial drug amount loaded in the gel and rms errors are indicated.

experimental concentration, respectively. The diffusivity for the each set of experimental dynamic concentration data was evaluated using the function 'fminsearch' in MATLAB. The value of D for DX was $1.00 \times 10^{-11} \pm 6.32 \times 10^{-13}$ m^2/s ($n = 10$). The theoretical profiles predicted by the model and the experimental data in drug loading experiments are given in Fig. 3. Two different theoretical profiles for the same initial concentration correspond to the two different gel volumes. The model predictions match the experimental data very well with the error ranging from 1.86 to 3.88%.

3.1.1.3. Dynamics of DX release. The dynamics of drug release from a gel into fresh solution can be described by Eq. (8) with boundary conditions (9), (10), and the following initial conditions

$$C_w(t = 0) = 0, \tag{11c}$$

$$C(t = 0, y) = C_i \tag{11d}$$

where C_i is an initial free drug concentration in the gel. If the gel properties do not change in the drug loading experiments, the values of K and D for drug release are expected to be the same as during the loading step. The numerical procedure described above was repeated with the release data to determine the drug diffusivity in the gel. The experimental data and the fitted profiles are plotted in Fig. 4. The amount of drug loading in the gel and the rms errors in the fit are also indicated in the figure. The model predictions match the experimental release data well with error range between 1.60 and 3.29%. The errors are slightly larger than those in drug loading, perhaps due to error accumulation to the previous drug loading experiments. From the fitting of the release data, the value of K and D for DX were determined to be 37.00 ± 3.41 and $1.06 \times 10^{-11} \pm 1.48 \times 10^{-12}$ m^2/s, respectively. These values are in excellent agreement with the values obtained from the loading data.

3.1.2. Release of the DX loaded in the gel by direct entrapment

3.1.2.1. Partition coefficient. Drugs can be loaded to the hydrogel contact lenses by soaking the gels in drug solutions, or by directly adding the drug to the polymerizing mixture (direct entrapment). While direct entrapment of drug may be more convenient, there is a possibility that a fraction of the drug may get irreversibly trapped in the gel. To investigate the feasibility of loading DX by direct entrapment, gels with different drug loading were prepared and drug release experiments were conducted from these gels. The release experiments were conducted with four different initial drug loadings ($M_0/M_g = 1.37$, 2.74, 4.78, and 6.82 mg/g). Each drug-laden gel was soaked in 3 ml of DI water (1st release). After equilibrium was achieved, the aqueous solution was replaced with 3 ml fresh DI water (2nd release). The 3rd release was conducted in the same manner.

The equilibrium concentration in the water phase can be used to determine the gel concentration by a using a mass balance, and then these can be used to determine the partition coefficients. In Table 2, the equilibrium concentrations in the water phase and the corresponding partition coefficients are listed. The values of K in Table 2 are significantly higher than the K values obtained above. Moreover, the K values for the 2nd release are much higher than those for the 1st release. Both of these effects could possibly be caused due to irreversible entrapment of a fraction of the drug. Based on this hypothesis, the mass balance in the drug-water system can be modified as

$$M_0 = V_w C_{w,f} + K V_g C_{w,f} = V_w C_{w,f} + (K' V_g C_{w,f} + M_p) \tag{12}$$

where M_0 is the total mass of drug loaded in the gel, M_p is the mass of drug that is irreversibly trapped in the gel, K' is the true partition coefficient of drug, and the other variables have the same definitions as above. The K values that were calculated by neglecting any irreversible entrapment are now called apparent partition coefficients ($\equiv K_{app}$) to differentiate them from the intrinsic partition coefficients K'. Based on the data obtained from the loading and release experiments from gels that had the

Table 2
Apparent partition coefficients (K_{app}), intrinsic partition coefficients (K'), and permanently entrapped drug amount (M_p) for DX release from the PHEMA gel synthesized in a direct entrapment method

No.	$C_{w,f}$ (mg/ml)	M_0/M_g (mg/g)	M_p/M_0 (%)	K_{app}	K'
1st release					
1	0.011	1.37	18.0	50.15	33.35
2	0.020	2.74	17.7	56.52	38.46
3	0.038	4.78	15.9	47.93	33.17
4	0.053	6.82	17.8	49.32	32.22
Average			17.4	50.98	34.30
2nd release					
1	0.005			75.82	
2	0.009			79.46	
3	0.016			69.11	
4	0.022			75.57	
Average				74.99	

drug loaded by soaking, it is reasonable to assume that the intrinsic partition coefficient is independent of concentration, and so for a given gel the K' values and also the M_p should be the same for the 1st and the 2nd releases. Using Eq. (12) for both the 1st and the 2nd releases, M_p and K' can be computed for each gel, and these are listed in Table 2. The values of K' (=34.30 ± 2.82) are in reasonable agreement with the values obtained from gels that were loaded by soaking in drug solutions. To further validate the results for K' and M_p, the apparent partition coefficient was determined by using the above equation for the 3rd release and the calculated values were in good agreement with the measured values. The results also show that about 17.4% of total drug loaded (Table 2) is permanently entrapped in the gel matrix and not available for the drug delivery. The permanent entrapment could be either physical entrapment in tightly bound regions or chemical entrapment due to reactions.

3.1.2.2. Dynamics of DX release. The model for the release of drug directly entrapped in the gel into the water is the same as that for the release of drug loaded by soaking. The initial concentration in the gel, which is a parameter required for the fit is set equal to the concentration of the drug that is available to diffuse. In Fig. 5, the experimental data for 1st and 2nd release are plotted along with the model predictions. The mean values of D for 1st and the 2nd releases are $1.00 \times 10^{-11} \pm 6.32 \times 10^{-13}$, and $1.23 \times 10^{-11} \pm 7.05 \times 10^{-13}$ m^2/s, respectively. The value of D obtained by fitting the 1st release data is in excellent agreement with the values reported above but the value increases by about 20% in the 2nd release. This is an unexpected result because the drug release in the first release step is not sufficiently large to impact the structure of the gel.

3.1.3. Effect of thickness of gel on DX loading

A major fraction of the drug present in the gel is bound to the polymer and so the drug transport may occur by a combination of surface and bulk diffusion. If surface diffusion rates are small, the bound drug could desorb and then diffuse via bulk diffusion. To determine whether transport of drug is controlled

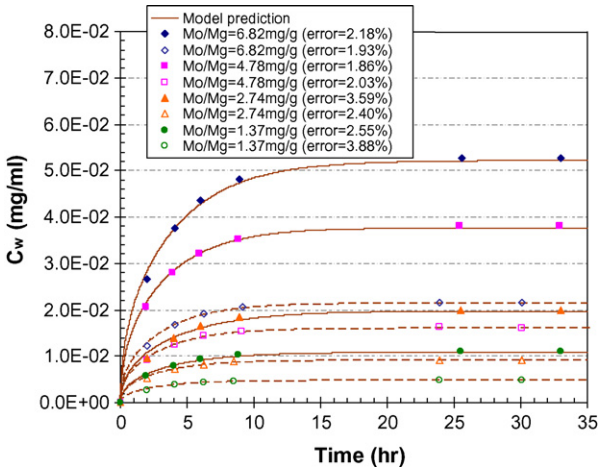

Fig. 5. Comparison of the model prediction and experimental data for DX release into the fresh water from PHEMA gels synthesized in a direct entrapment method. The solid legends and solid lines represent 1st release and the hollow legends and dashed lines 2nd release. $K' = 34.30 \pm 2.82$, D(1st release) $= 1.00 \times 10^{-11} \pm 6.32 \times 10^{-13}$ m^2/s, D(2nd release) $= 1.23 \times 10^{-11} \pm 7.05 \times 10^{-13}$ m^2/s, and $M_p/M_0 = 17.4 \pm 1.0$ % ($n = 4$). Initial drug amount loaded in the gel and rms errors are indicated.

by diffusion or by the process of adsorption–desorption of drug on the polymer, it was decided to fabricate gels with different thicknesses (0.1 and 0.2 mm thick in dry state). If the rate limiting step is diffusion, an increase in gel thickness by a factor of 2, while keeping fluid to gel ratio fixed, will increase the time scale of release by a factor of 4. A change in time scale by a factor of less than 4 signifies that the adsorption–desorption process occurs on a time scale comparable to the diffusion.

As described in methods section, both thick and thin gels were cut into square shaped pieces (about 1.5 cm × 1.5 cm) and unreacted monomer was removed by boiling. The gels were then dried and weighed and then soaked in water overnight for hydration. The hydrated thick gel ($H = 0.13$ mm) was put in 3 ml of DX–water solution and the hydrated thin gel ($H = 0.06$ mm) was put in 1.5 ml of DX–water solution for the drug loading studies.

The drug loading and release profiles from the thick and the thin gels are shown in Fig. 6. As mentioned above, if the drug transport is diffusion limited, the drug loading rate should be proportional to the square of the gel thickness. The ratio of gel to fluid volumes are not exactly equal for the two gels, and so to scale out the effect of the unequal volume ratio and the effect of the gel thickness, the dynamic drug concentration in water (C_w) was divided by final equilibrium drug concentration ($C_{w,f}$), and then this $C_w/C_{w,f}$ was plotted as a function of time/H^2. As seen in this figure, the profiles for the thick and the thin gels overlap both for loading and release experiments, which means that the drug release rate from the gel is exactly proportional to square of gel thickness, and thus the transport is diffusion limited. The values of K and D obtained by fitting the loading and the release data for the thick and the thin gels are noted in the figure caption.

3.1.4. Effect of crosslink density of gel on DX loading

To determine the effect of crosslink density on the DX transport, DX was directly entrapped into gels of four different

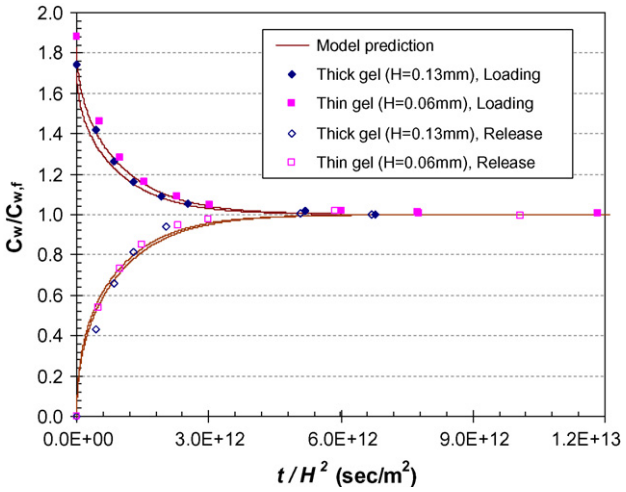

Fig. 6. The effect of gel thickness on DX loading and release of a PHEMA gel soaked in drug solution. Normalized DX loading and release profiles of thin gel and thick gel by final drug concentration in aqueous phase are plotted as a function of t/H^2. $C_{w,i} = 0.058$ mg/ml. For thick gel, K(loading) = 43.02 and D(loading) = 1.02×10^{-11} m^2/s (error = 1.93%), K(release) = 59.86 and D(release) = 1.22×10^{-11} m^2/s (error = 1.86%), for thin gel K(loading) = 44.44 and D(loading) = 9.51×10^{-12} m^2/s (error = 2.03%), K(release) = 53.85 and D(release) = 9.51×10^{-12} m^2/s (error = 4.93%). Half thicknesses of hydrated gels (H) are indicated.

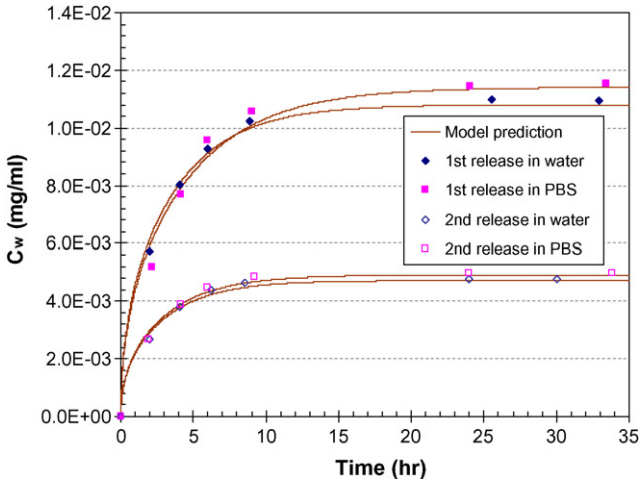

Fig. 7. The comparison of DX release profiles in water and PBS from a PHEMA gel synthesized in a direct entrapment method. $M_0/M_g = 1.37$ mg/g. For release in water, $K' = 33.35$, D(1st release) = 1.02×10^{-11} m^2/s (error = 2.55%), and D(2nd release) = 1.24×10^{-11} m^2/s (error = 3.88%), for release in PBS, $K' = 32.39$, D(1st release) = 9.21×10^{-12} m^2/s (error = 4.47%). and D(2nd release) = 1.17×10^{-11} m^2/s (error = 3.66%).

crosslink densities. The crosslink density is defined as

$$\text{crosslink density (\%)} = \frac{\text{mole of EGDMA added (mol)}}{\text{mole of HEMA added (mol)}} \times 100. \quad (13)$$

Since the gels were synthesized in a direct drug entrapment method, Eq. (12) can be applied to determine the intrinsic partition coefficient K' and the mass of drug permanently entrapped in the gel M_p, and these are listed in Table 3. There is no dependence of M_p/M_0 and K' on crosslink density. However, the diffusivity of drug decreases considerably with increasing crosslink density. The decrease in the diffusivity is likely the result of a decrease in the bulk diffusivity due to a decrease in the pore size of the gels.

3.1.5. DX release into PBS

All the results reported above for DX correspond to transport in gels hydrated in DI water. The transport in tear fluid or PBS which is a reasonable mimic of the tear fluid may be different from that in DI water partly because of differences in drug binding to the gel in the two mediums, and also due to different degree of swelling of gels, and also due to small differences in bulk viscosity. To investigate these issues, it was decided to load DX in PHEMA gels by direct entrapment, and measure the release rates in PBS and in DI water. The DX release profiles (both 1st and 2nd) in water and PBS were shown in Fig. 7. As seen in this figure, the two profiles are similar and the values of K and D, which are noted in the figure caption, are comparable as well. These results are expected because DX is a nonionic drug and so its partitioning is not expected to depend strongly on the salt concentration.

3.2. DXA loaded gel

Since DXA has a very low solubility in DI water and in PBS, it was loaded into the gel either by direct entrapment or by soaking in drug–ethanol solution. So the partition coefficients and diffusivities were only determined through the drug release experiments.

3.2.1. Release of the DXA loaded by direct entrapment

3.2.1.1. Partition coefficient and dynamics of DXA release. The release experiments were conducted with four different initial drug loadings ($M_0/M_g = 1.37$, 2.74, 4.78, and 6.82 mg/g). The equilibrium concentrations in the water phase and the corresponding values of the apparent partition coefficient K_{app} are listed in Table 4. Using Eq. (12), the intrinsic partition coefficient K' and the mass of drug permanently entrapped in the gel M_p were calculated and these are also given in Table 4. The intrinsic partition coefficient K' of DXA in PHEMA gel is also relatively independent of concentration,

Table 3
Effect of crosslink density on partition coefficient and diffusivities of DX in the gel synthesized in a direct drug entrapping method

Crosslink density (mol%)	M_0/M_g (mg/g)	M_p/M_0 (%)	$K_{1st\ release}$	$K_{2nd\ release}$	K'	$D_{1st\ release}$ (m^2/s)	$D_{2nd\ release}$ (m^2/s)
0.24	4.78	16.1	48.64	75.82	33.48	1.12×10^{-11}	1.22×10^{-11}
0.48	4.77	16.4	49.56	79.46	33.65	1.01×10^{-11}	1.13×10^{-11}
1.19	4.71	16.7	50.88	69.11	33.94	8.92×10^{-12}	9.08×10^{-12}
2.38	4.63	18.3	49.39	75.57	32.71	5.87×10^{-12}	6.53×10^{-12}

Table 4
Apparent partition coefficients (K_{app}), intrinsic partition coefficients (K'), and permanently entrapped drug amount (M_p) for DXA release from the PHEMA gel synthesized in a direct entrapment method

No.	$C_{w,f}$ (mg/ml)	M_0/M_g (mg/g)	M_p/M_0 (%)	K_{app}	K'
1st release					
1	0.0029	1.37	65.81	310.36	76.29
2	0.0053	2.74	68.09	339.17	76.55
3	0.0095	4.78	66.39	329.52	80.70
4	0.0136	6.82	65.42	330.19	85.76
Average			66.43	327.31	79.82
2nd release					
1	0.0018			449.32	
2	0.0033			498.77	
3	0.0061			469.17	
4	0.0090			453.99	
Average				467.81	

and its value is 79.82 ± 4.44 which is much higher than that of DX (34.30 ± 2.82). For DXA, only about 33.6% of initial drug is available for drug release since most of drug (66.4% of initial drug loading) is permanently entrapped. The D for the 1st and the 2nd releases are $1.29 \times 10^{-11} \pm 3.67\ 10^{-13}$ and $1.08 \times 10^{-11} \pm 1.13 \times 10^{-13}$ m^2/s, respectively, which are comparable to that for DX. As in Fig. 8, the overall time of DXP release is about 32 h which is longer than that of DX (about 16 h) even though they have comparable diffusivities since the time scale of diffusion is $K'\ H^2/D$ and K' value of DXA is about 2 times of that of DX. Since both DX and DXA have comparable sizes, the bulk diffusivity of these two molecules is expected to be similar. Furthermore, the effective diffusivity D values are also comparable even though the K' value differ by a factor of larger than 2 suggesting that the dominant transport mechanism is bulk diffusion, or alternatively the surface diffusivity is larger for DX by a factor of 2 and so the increased partition coefficient for DXA is balanced by a decrease in surface diffusivity leading to similar effective diffusivities for DX and DXA.

3.2.2. Release of the DXA loaded in the gel by presoaking in DXA–ethanol solution

As shown above, direct entrapment of DXA results in about 67% irreversible entrapment. To avoid losing a large fraction of the loaded drug to permanent entrapment, drug DXA was loaded in the gels by soaking in drug–ethanol solution. Release experiments from gels loaded with DXA by soaking are described below.

3.2.2.1. Effect of thickness of gel on DXA release. DXA release profiles from thick gel ($H = 0.13$ mm) and thin gel ($H = 0.06$ mm) are shown in Fig. 9. In this figure, $C_w/C_{w,f}$ is plotted as a function of time/H^2 to scale out the effects of changes in volume ratio of gel and water and gel thicknesses. The scaled release profiles overlap and the fitted values of D are 1.12×10^{-11} and 1.16×10^{-11} m^2/s for the thick and the thin gels, respectively, which both are in reasonable agreement with the values obtained from the direct entrapment studies. Based on the fact that transport time scales are quadratic in thickness, it can be concluded that DXA transport in the PHEMA gels is also diffusion limited.

3.2.2.2. DXA release into PBS. To mimic the transport of DXA in the tear fluid, release studies into PBS were done and compared with that in water (Fig. 10). The results show that DXA transport is slightly faster in gels soaked in PBS compared to those soaked in DI water. The fitted K and D values of DXA for PBS are 85.49 and 1.20×10^{-11} m^2/s, respectively, which are about 10% larger than those for DI water (82.79 and 1.12×10^{-11} m^2/s). Therefore, it can be concluded that the ionic strength and pH have a negligible effect on transport of

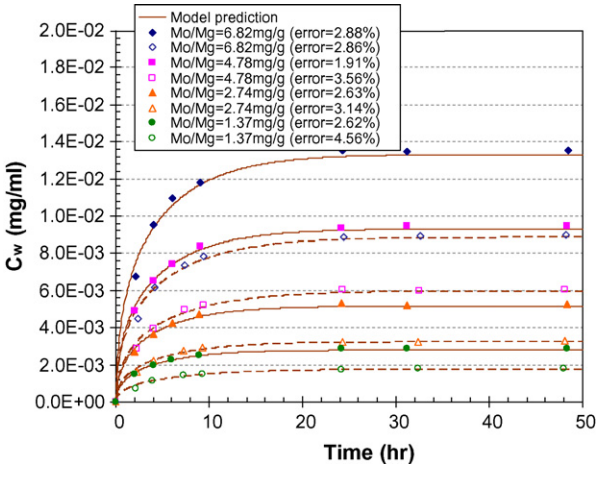

Fig. 8. Comparison of the model prediction and experimental data for DXA release into the fresh water from PHEMA gels synthesized in a direct entrapment method. The solid legends and solid lines represent 1st release and the hollow legends and dashed lines 2nd release. $K' = 79.82 \pm 4.44$, D(1st release) $= 1.29 \times 10^{-11} \pm 3.67 \times 10^{-13}$ m^2/s, D(2nd release) $= 1.08 \times 10^{-11} \pm 1.13 \times 10^{-13}$ m^2/s, and $M_p/M_0 = 66.4 \pm 1.2\%$ ($n = 4$). Initial drug amount loaded in the gel and rms errors are indicated.

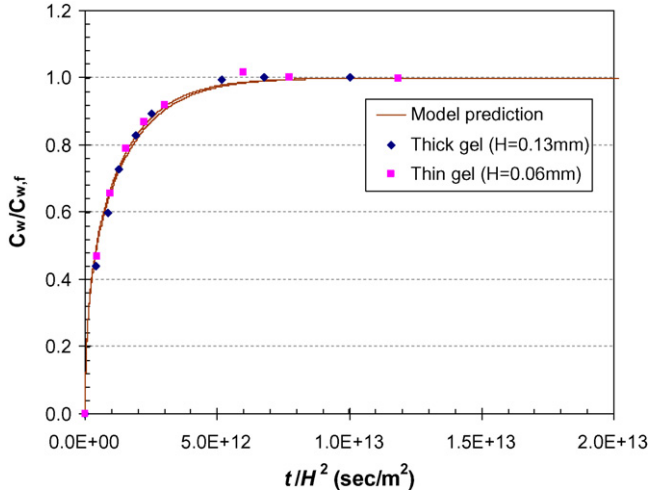

Fig. 9. The effect of gel thickness on DXA release of a PHEMA gel which has been soaked in DXA–ethanol solution. Normalized DXA release profiles of thin gel and thick gel by final drug concentration in aqueous phase are plotted as a function of t/H^2. $M_0/M_g = 1.76$ mg/g. For thick gel, $K = 85.49$ and $D = 1.12 \times 10^{-11}$ m^2/s (error = 2.09%), for thin gel $K = 85.79$ and $D = 1.16 \times 10^{-11}$ m^2/s (error = 2.58%). Half thicknesses of hydrated gels (H) are indicated.

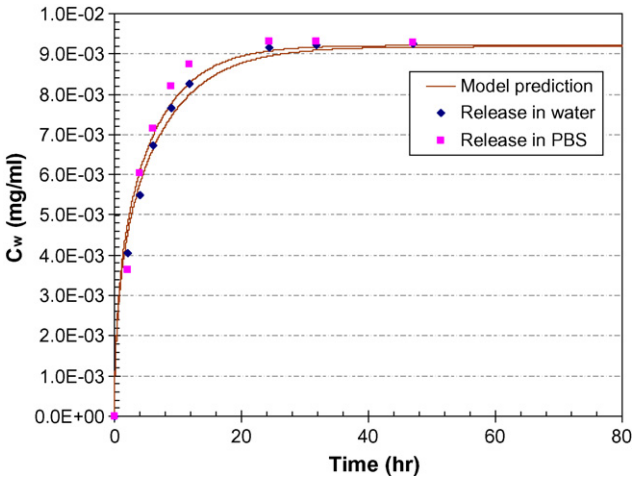

Fig. 10. The comparison of DXA release profiles in water and PBS from a PHEMA which has been soaked in DXA–ethanol solution. $M_0/M_g = 1.76$ mg/g. For release in water, $K = 85.49$ and $D = 1.12 \times 10^{-11}$ m^2/s (error = 2.09%), for release in PBS, $K = 82.79$ and $D = 1.28 \times 10^{-11}$ m^2/s (error = 2.58%).

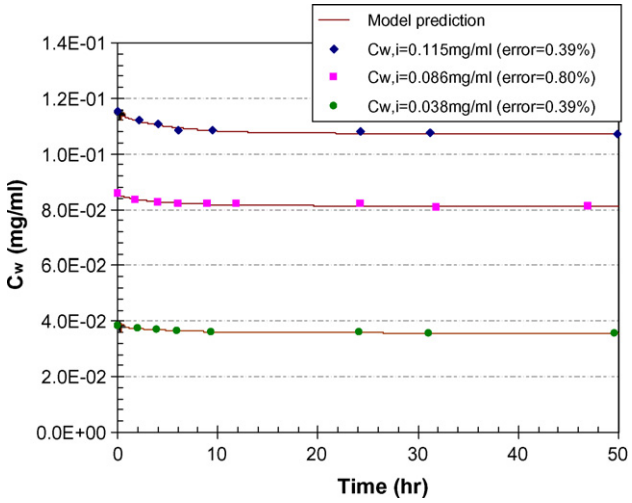

Fig. 11. Comparison of the model prediction and experimental data for DXP loading by PHEMA gel soaked in DXP solution. $K = 3.30 \pm 0.15$ and $D = 1.14 \times 10^{-12} \pm 8.98 \times 10^{-14}$ m^2/s ($n = 3$). Initial drug concentration in the aqueous phase and rms errors are indicated.

DXA, which is perhaps due to the fact that DXA is a nonionic drug.

3.3. DXP loaded gel

3.3.1. DXP loading and release studies

3.3.1.1. Partition coefficient and dynamics of DXP loading and release. The partition coefficients of DXP between the gel and the aqueous phase were determined by following the same procedures as described earlier for DX. DXP can get ionized with two pK_as of 1.89 and 6.4 (Banga, 1998) and so its behavior in DI water is expected to be significantly different from that in PBS. Accordingly, all the loading and release experiments for DXP were conducted in PBS in which a majority of the drug is expected to be charged because the pH ranges from 7.0 to 7.5. Drug loading studies were conducted by soaking gels in DXP-PBS solution at 0.115, 0.086, and 0.038 mg/ml. After equilibrium was attained, the PBS was replaced and the release experiments were conducted. The K values obtained from DXP loading and release are listed in Table 5. The K values from the loading experiments are relatively similar and the K values from the release experiments are similar, but these are larger than

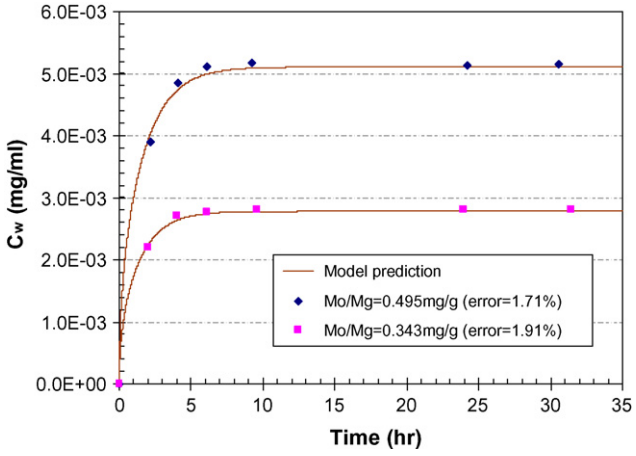

Fig. 12. Comparison of the model prediction and experimental data for DXP release into the PBS from a PHEMA gels which have been soaked in drug solution. Mean $K = 28.98$ and mean $D = 2.12 \times 10^{-11}$ m^2/s. Initial drug amount loaded in the gel and rms errors are indicated.

the loading K values by an order of magnitude. It is expected that if experiments are conducted in which the equilibrium concentrations are in between 0.005 and 0.036 mg/ml, the partition coefficients will transition smoothly from about 30 to 3. This

Table 5
DXP concentration and partition coefficients (K) of DXP in a soaking method

No.	$C_{w,f}$ (mg/ml)	$C_{w,i}$ (loading) (mg/ml)	M_0/M_g (release) (mg/g)	K
Loading				
1	0.036	0.038		3.33
2	0.081	0.086		3.14
3	0.107	0.115		3.44
Average				3.30
1st release				
2	0.0030		0.343	29.83
3	0.0052		0.495	28.13
Average				28.98

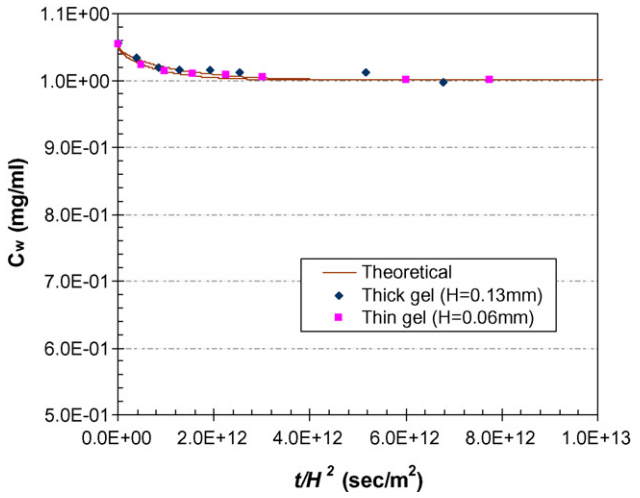

Fig. 13. The effect of gel thickness on DXP loading to a PHEMA soaked in DXP solution. Normalized DXP loading profiles for thin gel and thick gel by final drug concentration in aqueous phase are plotted as a function of t/H^2. $C_{w,i}$ = 0.086 mg/ml, For thick gel, $K = 3.14$ and $D = 1.21 \times 10^{-12}$ m^2/s (error = 0.80%), for thin gel $K = 2.89$ and $D = 1.35 \times 10^{-12}$ m^2/s (error = 0.23%). Half thicknesses of hydrated gels (H) are indicated.

behavior suggests that there may be two types of adsorption sites on the gel, and the first type binds the drug strongly but saturates at rather small concentrations. Since the K values in the release experiments are relatively concentration independent, the model proposed in Section 3.1.1.2 can still be used to determine the diffusivities for DXP loading into PHEMA gel. In the loading experiments the concentration inside the gel is close to zero at short times and so in principle the dependence of K on concentration needs to be taken into account to determine the diffusivity. However since K becomes concentration independent at relatively small concentrations we neglect this issue and use constant values of K from the loading experiments to fit the dynamic loading data. Some simulations were conducted by fitting the partition coefficient–concentration data to a sum of two Langmuir isotherms and then using this form in the model. However these simulations yielded diffusivities close to those obtained by using a constant value of K. The experimental profiles for loading and release and those predicted by model for DXP loading are plotted in Figs. 11 and 12. The fitted value of D from DXP loading is $1.14 \times 10^{-12} \pm 8.98 \times 10^{-14}$ m^2/s, which is an order of magnitude lower than that of DX or DXA loading. Furthermore the fitted value of D from the release data is 2.12×10^{-11} m^2/s, which is much larger than diffusivity obtained from the loading experiments. The differences between the diffusivities in loading and release can be explained by noting that the fitted values represent the average diffusivities, and include contributions from both bulk diffusion and surface diffusion, i.e., $D = fD_f + D_s(K - f)$. The values of D_s and D_f are likely to be independent of drug concentrations but the partition coefficient could depend on concentration. So concentration dependence of the effective diffusivity likely arises from the surface diffusion. For the case of DXP, the partition coefficients at release concentrations are an order of magnitude larger than those in the loading concentrations and D is also an order of magnitude larger, suggesting that the surface diffusion may be the dominant mechanism for transport of dexamethasone phosphate. It is noted though that this is only a plausible argument and we cannot conclusively prove this hypothesis with the indirect measurements reported in this paper.

3.3.1.2. Effect of thickness of gel on DXP loading. The effect of gel thickness on DXP transport was investigated by performing DXP loading experiments at initial concentration 0.086 mg/ml with hydrated gels of two different thicknesses (half thickness $H = 0.13$ and 0.06 mm). The scaled $C_w/C_{w,f}$ vs. time/H^2 profiles are plotted Fig. 13. The two loading profiles are relatively similar, and the fitted values of K (3.14 for thick and 2.89 for thin) and D (1.21×10^{-12} m^2/s for thick and 1.35×10^{-12} m^2/s for thin) are also in reasonable agreement suggesting that the process of DXP transport is also diffusion limited.

3.3.1.3. Effect of ionic strength of outer solution on DXP loading and release. The molecular weight of DXP (516.4) is only marginally larger than those of DX (392.5) and DXA (434.5) but one significant difference between DXP and the other two forms of dexamethasone is the fact that DXP exists in charged form in PBS. To investigate whether electrostatic effects contribute to the differences in diffusivities between the three forms of dexamethasone, the transport of DXP was investigated in NaCl-PBS solutions with different ionic strengths (I = 173, 594, 1022 and 1202 nm). Initial concentration of DXP ($C_{w,i}$) was fixed at 0.087 mg/ml in each of the solutions. The DXP loading and release profiles for these experiments are shown in Fig. 14. To

Table 6
Effect of ionic strength (I) on DXP loading and release

No.	I (mM)	$C_{w,f}$ (mg/ml)	$C_{w,i}$ (loading) (mg/ml)	M_0/M_g (release) (mg/g)	K	D ($\times 10^{-12}$ m^2/s)
Loading						
1	173	0.0816	0.0857	0.343	2.87	1.44
2	594	0.0797	0.0857	0.490	4.33	0.82
3	1022	0.0785	0.0857	0.522	5.30	0.47
4	1202	0.0776	0.0857	0.635	6.08	0.39
Release						
1	173	0.0031			19.52	19.76
2	594	0.0041			26.49	12.10
3	1022	0.0047			31.56	4.53
4	1202	0.0047			42.76	3.27

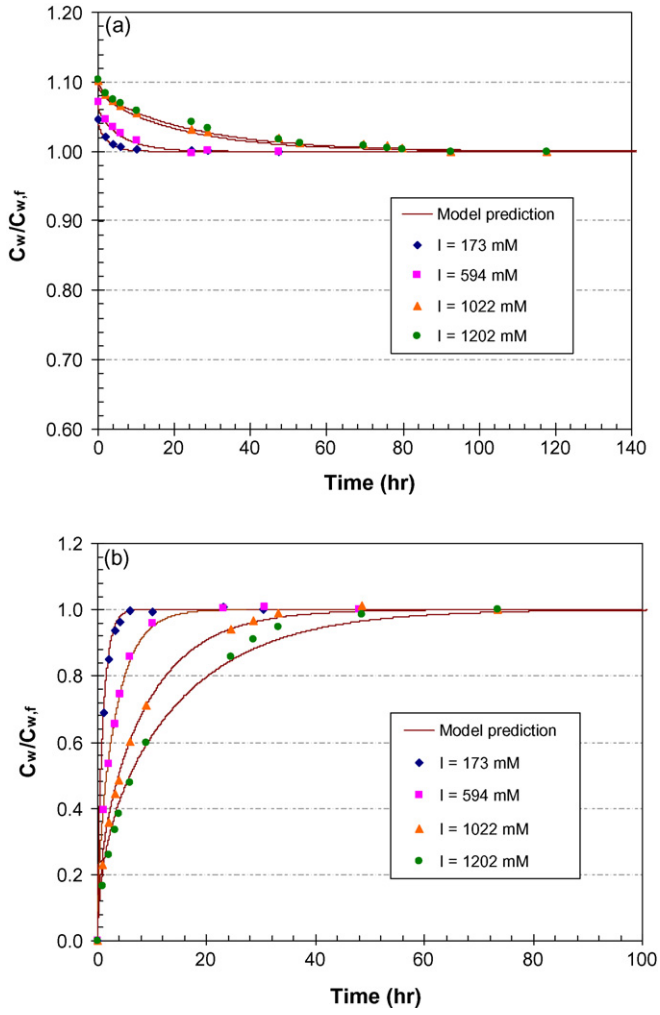

Fig. 14. Effect of ionic strength on DXP loading and release in a soaking method. (a) Normalized DXP loading profiles by final drug concentration in outer solution with different ionic strength. (b) Normalized DXP release profiles by final drug concentration in outer solution. $C_{w,i} = 0.086$ mg/ml for loading. Ionic strength is indicated.

clearly observe the effect of ionic strength on loading and release timescale, the DXP concentration in aqueous phase was normalized by final equilibrium concentration and plotted in Fig. 14(a and b), for the loading and release, respectively. It is clearly evident that an increase in the ionic strength leads to an increase

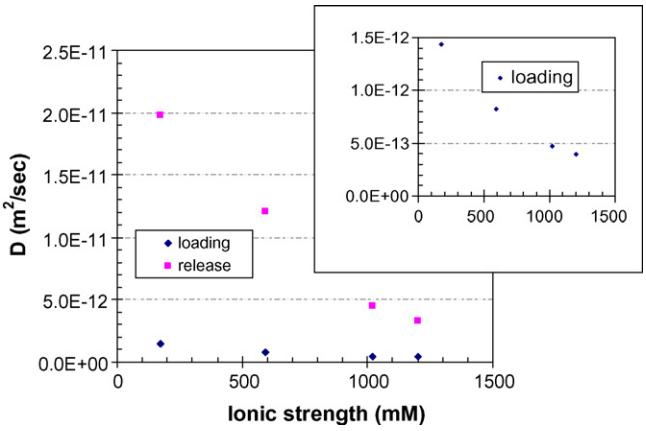

Fig. 15. The plot of diffusivities of DXP for loading and release in a soaking method as a function of ionic strength. $C_{w,i} = 0.086$ mg/ml.

in time needed to achieve equilibrium during both the loading and the release phases. The fitted values of K and D are listed for these experiments in Table 6. The values of K are relatively independent of the ionic strength but the values of D for both the loading and the release decrease with increasing ionic strength. This tendency can be seen more clearly in Fig. 15 which plots the diffusivities of DXP for loading and release as a function of the ionic strength. The changes in D with ionic strength suggest that electrostatics affect the transport of charged drugs like DXP even in PBS. The effect of electrostatics is expected to reduce with increasing ionic strength due to screening effects and so the D values at the very high ionic strength are expected to be the true diffusivity values. The D values at the highest ionic strength are similar from both loading and release but these are an order of magnitude lower compared to the diffusivities of the uncharged forms of dexamethasone described earlier.

In an effort to understand the mechanisms of transport of charged drugs, it was decided to explore transport of timolol maleate, which also exists in a charged form at physiological pH and its molecular weight is comparable to that of dexamethasone phosphate. Transport of timolol maleate in PHEMA and other types of hydrogels has been investigated by a number of researchers. However, to our knowledge the effect of ionic strength on transport of timolol maleate in PHEMA hydrogels has not been investigated. We conducted loading experiments for timolol maleate at a fixed loading concentration of 0.0857 mg/ml

Table 7
Effect of ionic strength on timolol maleate loading and release

No.	I (mM)	$C_{w,f}$ (mg/ml)	$C_{w,i}$ (loading) (mg/ml)	M_0/M_g (release) (mg/g)	K	D ($\times 10^{-12}$ m^2/s)
Loading						
1	173	0.0779	0.0857	0.594	5.66	5.66
2	594	0.0795	0.0857	0.472	4.41	4.79
3	1022	0.0788	0.0857	0.529	4.99	2.79
4	1202	0.0788	0.0857	0.525	4.95	2.57
Release						
1	173	0.0069			7.72	19.62
2	594	0.0056			6.38	13.12
3	1022	0.0058			11.31	12.75
4	1202	0.0060			8.79	6.90

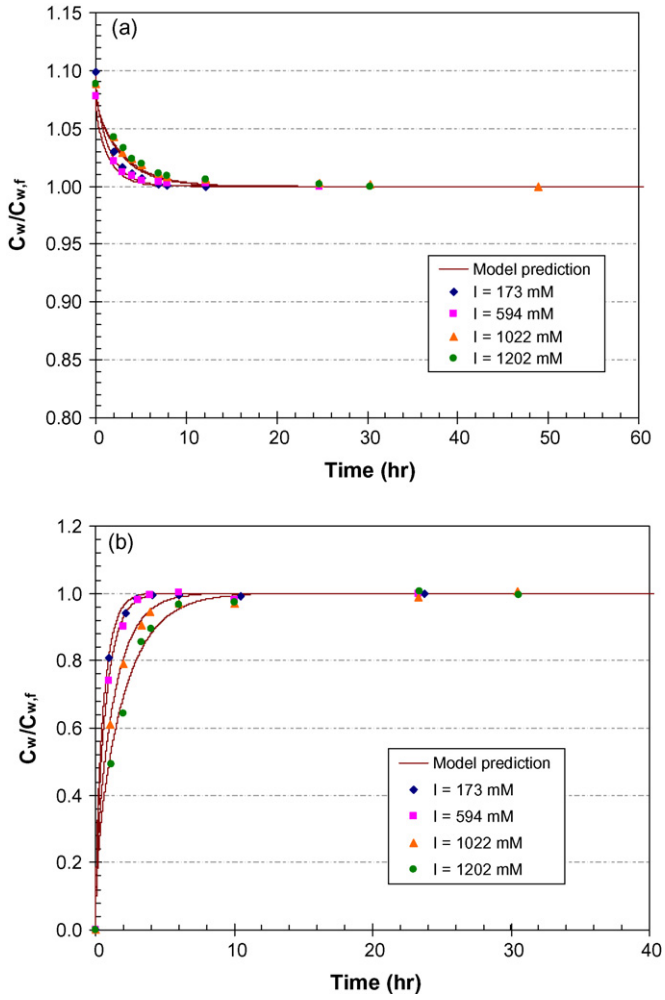

Fig. 16. Effect of ionic strength on timolol maleate loading and release in a soaking method. (a) Normalized timolol maleate loading profiles by final drug concentration in outer solution. (b) Normalized timolol maleate release profiles by final drug concentration in outer solution. $C_{w,i} = 0.086$ mg/ml for loading. Ionic strength is indicated.

and at three different salt concentrations with protocols identical to those for dexamethasone phosphate. Subsequently, release experiments were performed also with protocols described earlier for dexamethasone phosphate. The loading and release data was fit in the same manner as described earlier. The results of loading and release experiments along with the fitted curves and the best fit values of diffusivities are shown in Fig. 16 and Table 7. Timolol maleate diffusivities obtained by fitting the loading data are different from those obtained by fitting the release data. Furthermore, the diffusivities decrease with an increase in ionic strength and at the highest ionic strength the diffusivities from the loading and the release are similar (Fig. 17). Each of these trends is similar to those for dexamethasone phosphate. However, the values of diffusivities obtained for timolol are much larger than those for dexamethasone phosphate. At the highest ionic strength where electrostatics are expected to be screened, the partition coefficients for timolol maleate during the release is about 60% higher than that during loading, and the diffusivities are about twice, which is in accordance

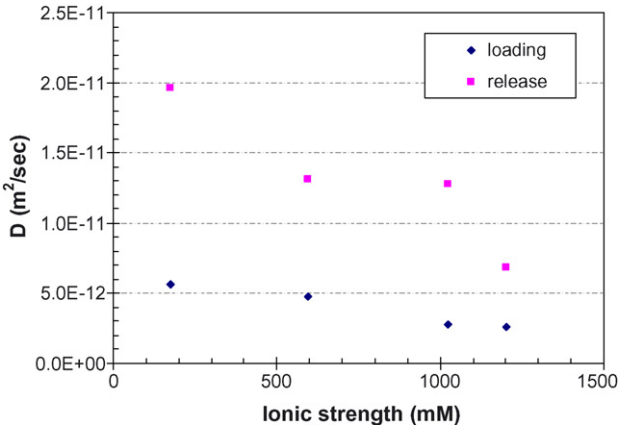

Fig. 17. The plot of diffusivities of timolol maleate for loading and release in a soaking method as a function of ionic strength. $C_{w,i} = 0.086$ mg/ml.

with the earlier observations for other drugs. However the values of diffusivities for timolol maleate during loading are about 5 times that of DXP even though the partition coefficients are comparable.

We speculate that the significant reduction in diffusivity of DXP may be due to aggregation of the charged drug into micelles. Since DXP is a relatively linear molecule with a charged hydrophilic group on one side and the hydrophobic group on the other, it is reasonable to expect DXP to be surface active and also form micelles. In fact corticosteroid 21-phosphate esters including DXP have been reported to form micelles in DI water and methylprednisolone 21-phosphate whose structure is very similar to that of DXP forms micelles above a concentration of 0.017 M (Flynn and Lamb, 1970). To verify whether DXP forms micelles at concentrations corresponding to drug loading and release experiments, the surface tension isotherm of DXP in PBS was measured. The surface tension vs. log (concentration) data plotted in Fig. 18 demonstrates that the CMC of DXP in PBS is above 0.1 M, which is higher than the concentrations explored in the loading-release studies. Thus aggregation of DXP into micelles is an unlikely reason

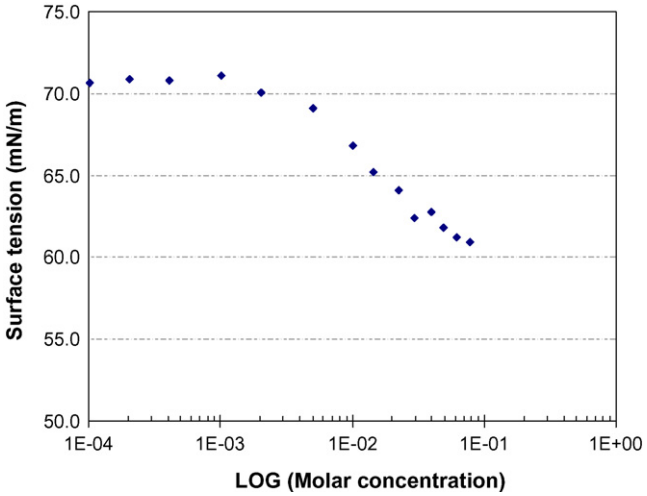

Fig. 18. The plot of surface tension of DXP as a function of concentration for determination of CMC.

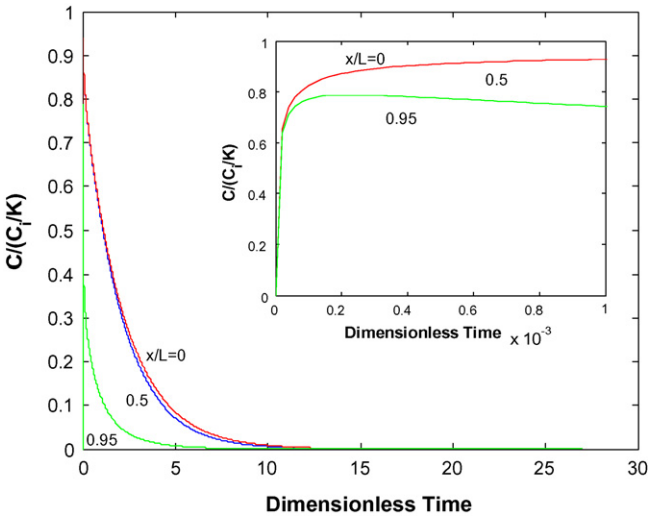

Fig. 19. DX concentration transients in the POLTF at different axial locations for case 1, i.e., no flux to the PLTF. The inset shows a magnified view near $t = 0$. The values of P1, P2, and P3 are 0.138, 321.8, and 173.2, respectively.

for the small diffusivities. The mesh size of the PHEMA hydrogel was obtained by following the reported method by Canal and Peppas (1989). The mean value of the equilibrium volume degree of swelling of the PHEMA hydrogel is 1.60, and accordingly the corresponding mesh size is about 1.7 nm. The size of DXP is about 1.2 nm and this is comparable to the mesh size of PHEMA hydrogel. Aggregation of DXP micelles in the bulk phase in the gel is again unlikely the case for this reason.

3.4. Mathematical model for drug transport to the cornea

3.4.1. Model for drug release from the contact lens into the eye

We utilized the model for drug delivery by soaked contact lenses reported previously (Li and Chauhan, 2006) and detailed description is in Appendix A. Below we solve the coupled mass transfer problem for drug delivery from a contact lens in the eye.

3.4.1.1. Concentration profiles in the POLTF. Fig. 19 shows DX concentration in the post-lens tear film vs. time plots at three axial locations for case 1, i.e., no flux to the pre-lens tear film. The inset in the figure shows the magnified view of the plots near $t = 0$. The concentration starts at lens center zero and then very quickly increases to a value of about 0.85. Since the concentrations are dedimensionalized by C_i/K, the maximum possible value of C_f in the POLTF is 1. During the period in which the concentration is increasing, the drug flux from the gel is larger than the sum of the drug loss from the sides ($x = \pm L$) to the outer tear lake and the drug uptake by the cornea. The maximum value of the concentration is reached in a very short period of time because the volume of the POLTF is small as reflected in the large value of P2. At initial times, the drug flux into the cornea and the drug loss from the sides are much less than the drug flux from the lens causing drug concentration in the post-lens tear film to increase. However, as the drug concentration in the POLTF builds up, the flux of the drug from the lens decreases and the drug loss from the sides due to dispersion and the drug flux into cornea increases. Consequently, very quickly, the drug concentrations in the POLTF begin to decrease.

3.4.1.2. Fraction of drug that enters cornea. The amount of drug that diffuses into the cornea is simply equal to $2\int_0^\infty \int_0^L k_c C_f \, dx \, dt$. The mass of drug that diffuses into the tear lake from the edges of the POLTF is given by $2\int_0^\infty -D_f D^* (dC_f/dx)|_{x=L} h_f \, dt$. Finally, the amount of the drug that is lost to the PLTF is given by $2\int_0^\infty \int_0^L D_g (dC_g/dy)|_{y=0} \, dx \, dt$. On dedimensionalizing each of these masses by the initial mass of drug in the gel ($=2C_i L h_g$), we get the following equations:

$$F_c = \frac{2}{M_0}\int_0^\infty \int_0^L k_c C_f \, dx \, dt = \frac{P3}{P2}\int_0^\infty \int_0^1 C_f \, d\eta \, d\tau \qquad (25)$$

$$F_s = \frac{2}{M_0}\int_0^\infty -D_f D^* \left.\frac{dC_f}{dx}\right|_{x=L} h_f \, dt = \frac{P1}{P2}\int_0^\infty D^* \left.\frac{dC_f}{d\eta}\right|_{\eta=1} d\tau \qquad (26)$$

$$F_p = \frac{2}{M_0}\int_0^\infty \int_0^L D_g \left.\frac{dC_g}{dy}\right|_{y=0} dx \, dt = \int_0^\infty \int_0^1 \left.\frac{dC_g}{d\zeta}\right|_{\zeta=0} d\eta \, d\tau \qquad (27)$$

where F_c is the fraction of the total drug that enters cornea, F_s is the fraction of the total drug wasted from the side to the outer tear lake, and F_p is the fraction of the total drug wasted to the PLTF.

After determining the concentration profiles, the various fractions can be determined by computing the integrals numerically. The values of F_c, F_s, and F_p are listed in Table 8 for the three drugs for both case 1 (no flux to PLTF) and case 2 (zero concentration in PLTF). The values of F_c represent the bioavailability and these are much higher than 1–3%, which are the typical values for delivery by eye drops. The values of F_c are higher for case 1 because of neglect of drug loss to the pre-lens tear film. The physiological boundary condition in the pre-lens tear film is expected to be in between case 1 and 2, and so the average of these two cases may be a good approximation for the bioavailability. Amongst the three drugs investigated here, the bioavailability is highest for DXA, primarily due to the highest cornea permeability.

Table 8
Various fractions (F_c, F_s, and F_p) in the eye for three derivatives of dexamethasone

	DX	DXA	DXP
Case 1 (no flux to PLTF)			
F_c	0.8291	0.9196	0.7893
F_s	0.1737	0.0799	0.2122
Case 2 (zero concentration in PLTF)			
F_c	0.1573	0.2912	0.0711
F_s	0.8171	0.7202	0.9068
F_p	0.0486	0.0298	0.0375

4. Conclusions

The bioavailability of ophthalmic drugs delivered via contact lenses is significantly higher in comparison to that for topical application as eye drops. The bioavailability of ophthalmic drugs delivered by contact lenses can be estimated by solving the mass transport problem in the eye in the presence contact lenses. In order to solve the transport model, one requires the parameters that describe the drug transport in the contact lens. In this paper we have investigated the transport of three different forms of dexamethasone in PHEMA gels, which are a common contact lens material.

The transport of the drugs is investigated by soaking PHEMA gels in aqueous drug solutions and monitoring the dynamic drug concentrations. After reaching equilibrium, the gels are soaked in fresh solutions for the release experiments. Since DXA has very limited aqueous solubility, it is loaded into the gel via soaking in ethanol–drug solution. Furthermore drug release studies are also conducted for situations in which the drug was added directly to the polymerizing mixture. The equilibrium concentrations in both the loading and the release studies are utilized to determine the partition coefficients. Furthermore, the dynamic data is fitted to the diffusion equation to determine the mean diffusivity, which includes contributions from both bulk and surface diffusion.

The partition coefficients of DX and DXA are independent of concentration, and are about 40 and 80, respectively. The partition coefficients are relatively similar from both the loading and the release studies. The partition coefficients estimated from the direct entrapment studies seem to be significantly different but the differences can be attributed to the fact that addition of drug to the polymerizing mixture results in some irreversible drug entrapment. The irreversible entrapment could be both physical and/or chemical. By utilizing the first, second and third release results, it was determined that about 17% of DX and 65% DXA gets irreversibly entrapped, and after taking into account the irreversible entrapment, the partition coefficients are in reasonable agreement with the results from soaking and release studies. The transport of all the three drugs is diffusion limited. The diffusivity of DX is 1.05×10^{-11} m^2/s from both the loading and the release studies, and the values are comparable in release studies with directly entrapped drug. The diffusivity for DXA is about 1.29×10^{-11} m^2/s, and this value too is similar for all uptake and release studies. There are slight differences in diffusivities estimated from the first and the second releases after direct entrapment, but these differences are within experimental errors.

The partition coefficient of DXP is concentration dependent; it decreases from about 30 to 3 as the concentration increase from 0.003 to 0.107 mg/ml. The diffusivity of DXP is larger for the release phase than for the loading phase by an order of magnitude, which can be explained by noting that the fitted values represent the average diffusivities, and include contributions from both bulk diffusion and surface diffusion, i.e., $D = fD_f + D_s(K - f)$. To investigate whether electrostatic effects impact DXP transport, the transport of DXP was investigated in NaCl–PBS solutions with different ionic strengths. These experiments show that the partition coefficient of DXP is relatively independent of the ionic strength but the mean diffusivity values decrease with an increase in ionic strength. At all ionic strengths, the diffusivity in loading is smaller by about a factor of 10, which can be attributed to the contribution from surface diffusion. The fact that diffusivities change on increasing ionic strength suggests that electrostatic effects are important in transport of charged drugs even in PBS. If there is screening effect of salt on charged drug, DXP, we can assume that D of DXP will be close to true diffusivity at very high ionic strength of outer solution which would be similar to that of the other noncharged derivatives, but obtained D at very high ionic strength was still as low as 10^{-12} m^2/s, an order of magnitude lower than that of the others.

The partition coefficient of timolol maleate, which is also charged in PBS is relatively independent of concentration and depends weakly on the ionic strength. Timolol maleate diffusivities obtained by fitting the loading data are different from those obtained by fitting the release data. At the highest ionic strength where electrostatics are expected to be screened, the partition coefficients for timolol maleate during the release is about 60% higher than that during loading, and the diffusivities are about twice, which could perhaps be attributed to surface diffusion. Furthermore, the diffusivities decrease with an increase in ionic strength and at the highest ionic strength the diffusivities from the loading and the release are similar. These trends are similar to those for dexamethasone 21-disodium phosphate but values of diffusivities for timolol maleate during loading are about 5 times that of DXP even though the partition coefficients are comparable.

We speculated that the significantly smaller diffusivity of DXP is due to aggregation of DXP into micelles. However surface tension measurements showed that the CMC of DXP in PBS is larger than concentrations explored in loading-release studies and so aggregation into micelles is unlikely to cause the reduction in diffusivities. It is however possible that DXP aggregates at lower concentrations into complex structures inside the PHEMA gel due to interactions with the polymer.

The predicted values of F_c, which represent the bioavailability, are much higher than the typical values for delivery by eye drops. The values of F_c are higher for case 1 because of neglect of drug loss to the pre-lens tear film. The physiological boundary condition in the pre-lens tear film is expected to be in between case 1 and 2, and so the average of these two cases may be a good approximation for the bioavailability. Amongst the three drugs investigated here, the bioavailability is highest for DXA, primarily due to the highest cornea permeability. Thus DXA delivery via soaked daily disposable PHEMA contact lenses seems like a much more efficient method of delivering dexamethasone to eyes in comparison to delivery through eye drops. However clinical tests are needed to firmly establish the safety and efficacy of drug-loaded contact lenses for ophthalmic drug delivery because issues such as continuous exposure of ocular tissue to the drug could possibly evoke toxic response.

Acknowledgement

This research is partly funded by support from the National Science Foundation (CTS 0426327).

Appendix A

Fig. 20 shows the real and the model geometry of the lens and the tear film. The post-lens tear film is pictured as a flat, two-dimensional film bounded by an undeformable cornea and an undeformable but moving contact lens. The lens is treated as a two-dimensional body of length L and thickness h_g, and is assumed to extend infinitely in the third direction. The post-lens tear film has a thickness h_f which may depend on x as the front surface of the eye has a complicated geometry, but for simplicity, is taken to be independent of x in this paper. The curvatures of the cornea and the lens have been neglected because the thicknesses of the tear film (about 10 μm) and of the contact lens (about 100 μm) are much smaller than the corneal radius of curvature of about 1.2 cm. The assumption of a two-dimensional geometry has been made to simplify the problem. The effect of gravity is negligible in the POLTF. Thus, for our purposes the pre-lens tear film–contact lens–POLTF–cornea system is a flat, horizontally oriented channel. These assumptions have been utilized in the past to model mass transfer in the POLTF (Fig. 20). The drug concentrations in the gel matrix of the contact lens, and the tear film are C_g and C_f, respectively. The time $t=0$ corresponds to insertion of the lens in the eye, and so the initial concentration in the tear film is zero, and the initial concentration in the lens is the concentration obtained in the loading phase, which is now defined as C_i. To determine the drug flux to the cornea, we need to simultaneously solve the modified diffusion equation in the gel matrix and the convection diffusion equation in the pre and the post-lens tear film.

By using asymptotic techniques, and multiple time scale analysis, the transport problem in the post-lens tear film can be simplified to a dispersion equation of the form

$$\frac{\partial C_f}{\partial t} = \frac{\partial}{\partial x} D^* \frac{\partial C_f}{\partial x} + \frac{j - k_c C_f}{h_0} \tag{A.1}$$

where D^* is the effective dispersion coefficient, k_c is the permeability of the cornea for the drug and j is the flux of the drug entering the post-lens tear film from the contact lens, which is determined below by solving the transport problem in the lens. The details of this derivation of Eq. (A.1) are available in Ref. Li and Chauhan (2006). Also the expression for the dispersion coefficient, which depends on the motion of the contact lens that is caused by the blinks, is also available in Ref. Li and Chauhan (2006).

As described in the previous section, the transport problem in the gel is

$$\frac{\partial (KC)}{\partial t} = D \frac{\partial^2 C}{\partial y^2} \tag{A.2}$$

Since the value of partition coefficient is constant for timolol release in PBS, the above equation can be expressed as

$$\frac{\partial C_g}{\partial t} = D_e \frac{\partial^2 C_g}{\partial y^2} \tag{A.3}$$

where $D_e \equiv D/K$, and $C_g = KC$ is the drug concentration in the gel. The above equation is subjected to the following boundary conditions,

$$C_g(y = h_g) = KC_f(x) \tag{A.4a}$$

$$-D_e \frac{\partial C_g}{\partial y} = j \tag{A.4b}$$

$$\frac{\partial C_g}{\partial_y}(y = 0) = 0 \tag{A.4c}$$

The boundary condition (A.4a) assumes equilibrium between the concentration in the contact lens and that in the tear fluid in the POLTF and Eq. (A.4b) imposes flux continuity, and thus couples the mass transfer problems in the POLTF and in the contact lens. The boundary condition (A.4c) assumes that there is no loss of drug from the lens to the pre-lens tear film (PLTF) that lies in between the lens and the air. This assumption may be reasonable because the PLTF breaks very rapidly and the breakup of the PLTF prevents any further drug loss from the front surface. Additionally, the PLTF breakup causes partial dehydration of the lens in the region close to the front surface, and consequently the front surface of the contact lens is expected to be glassy, which may further reduce drug flux from the front surface. This is clearly the scenario that will maximize the fraction of the drug trapped in the lens that will eventually be delivered

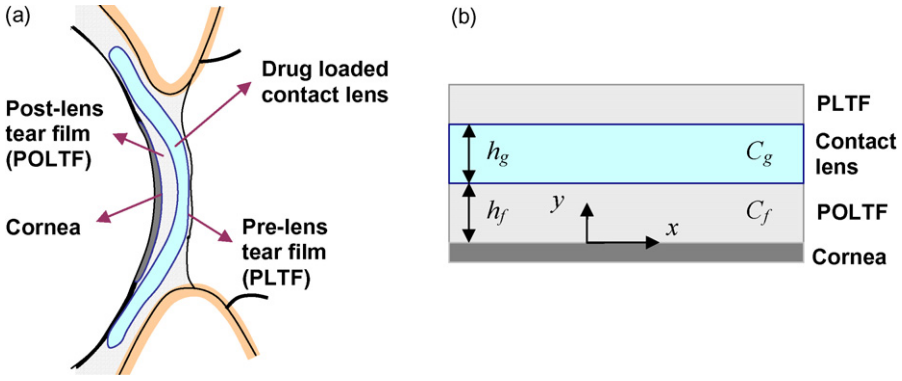

Fig. 20. (a) The real geometry utilized in the model for the PLTF-lens-POLTF system. (b) The idealized geometry.

Table 9
Model parameters for three derivatives of dexamethasone

		DX	DXA	DXP
K		32.18	82.79	28.98
D_e (m^2/s)		2.92×10^{-13}	1.55×10^{-13}	7.32×10^{-13}
D_f (m^2/s)		4.03×10^{-10}	3.64×10^{-10}	3.06×10^{-10}
k_c (m/s)[a]		5.06×10^{-8}	2.11×10^{-7}	3.87×10^{-8}
P1		0.138	0.235	0.042
P2		321.8	827.9	289.8
P3		173.2	1364.7	52.9
L (cm)	1			
h_g (μm)	100			
h_f (μm)	10			

[a] Civiale et al. (2004).

to the cornea. This extreme case in which the drug flux to PLTF is neglected is referred as case 1. To determine the fraction of trapped drug that will go to the cornea for the other extreme, we investigate the case in which we assume that the drug can diffuse into the PLTF and that rapid mixing and drainage from the PLTF keeps the drug concentration in PLTF about zero. This case is referred as case 2, and for this case, the boundary condition Eq. (A.4c) is replaced by the following equation

$$C_g(y = 0) = 0 \tag{A.5}$$

Finally the initial conditions for the tear film and the contact lens are:

$$C_f(t = 0) = 0, \qquad C_g(t = 0) = C_i \tag{A.6}$$

The dimensionless forms of the equations are:

$$\frac{\partial \tilde{C}_f}{\partial \tau} = \mathrm{P1}\frac{\partial}{\partial \eta}\tilde{D}^*\frac{\partial C_f}{\partial \eta} + \mathrm{P2} \times \tilde{j} - \mathrm{P3} \times \tilde{C}_f \tag{A.7}$$

where $\tau \equiv D_e t/h_g^2$, $\tilde{D}^* = D^*/D$, $\eta \equiv x/L$, $\tilde{C}_f \equiv (C/(C_i/K))$, $\mathrm{P1} = D_f h_g^2/D_e L^2$, $\mathrm{P2} = K(h_g/h_f)$, $\mathrm{P3} = k_c h_g^2/h_f D_e$, and $\tilde{j} \equiv (j/(D_e C_i/h_g))$ is the dimensionless flux from the contact lens into the POLTF. By using convolution theorem (Li and Chauhan, 2006) the gel problem can be solved to yield the following expressions for the dimensional flux for case 1 and 2,

$$\tilde{j} = 2\sum_{n=0}^{\infty} e^{-(2n+1)^2\pi^2\tau/4} + 2\sum_{n=0}^{\infty}\left(\int_0^{\tau} \tilde{C}_f(\tau^*)\frac{(2n+1)^2\pi^2}{4} e^{-(2n+1)^2\pi^2(\tau-\tau^*)/4}\, d\tau^* - C_f(\tau)\right) \tag{A.8}$$

$$\tilde{j} = \sum_{n=0}^{\infty} 4\, e^{-(2n+1)^2\pi^2\tau} - \tilde{C}_f(\tau) + 2\sum_{n=0}^{\infty}\left(\int_0^{\tau} \tilde{C}_f(\tau^*) n^2\pi^2\, e^{-n^2\pi^2(\tau-\tau^*)}\, d\tau^* - \tilde{C}_f(\tau)\right) \tag{A.9}$$

The values of the dimensional parameters required to calculate P1, P2 and P3 are noted in Table 9. The parameters D_e and K are the values determined above by fitting the dynamic concentration data in loading and release experiments to a model, and the other parameters are obtained from literature. The values of P1, P2 and P3 for the transport of the three drugs are noted in Table 9.

References

Ahmed, I., Patton, T.F., 1985. Importance of the noncorneal absorption route in topical ophthalmic drug delivery. Invest. Ophthalmol. Vis. Sci. 26, 584–587.

Ahmed, I., Patton, T.F., 1987. Disposition of timolol and inulin in the rabbit eye following corneal versus non-corneal absorption. Int. J. Pharm. 38, 9–21.

Arthur, B.W., Hay, G.J., Wasan, S.M., Willis, W.E., 1983. Ultrastructural effects of topical timolol on the rabbit cornea—outcome alone and in conjunction with a gas permeable contact-lens. Arch. Ophthalmol. 101, 1607–1610.

Banga, A.J., 1998. Electrically Assisted Transdermal and Topical Drug Delivery. Taylor & Francis, Bristol.

Canal, T., Peppas, N.A., 1989. Correlation between mesh size and equilibrium degree of swelling of polymeric networks. J. Biomed. Mater. Res. 23, 1183–1193.

Civiale, C., Bucaria, F., Piazza, S., Peri, O., Miano, F., Enea, V., 2004. Ocular permeability screening of dexamethasone esters through combined cellular and tissue systems. J. Ocul. Pharmacol. Ther. 20, 75–84.

Clark, A.F., Yorio, T., 2003. Ophthalmic drug discovery. Nat. Rev. Drug Discov. 2, 448–459.

Colombo, P., Bettini, R., Peppas, N.A., 1999. Observation of swelling process and diffusion front position during swelling in hydroxypropyl methyl cellulose (hpmc) matrices containing a soluble drug. J. Controlled Release 61, 83–91.

Creech, J.L., Chauhan, A., Radke, C.J., 2001. Dispersive mixing in the posterior tear film under a soft contact lens. Ind. Eng. Chem. Res. 40, 3015–3026.

Einmahl, S., Zignani, M., Varesio, E., Heller, J., Veuthey, J.L., Tabatabay, C., Gurny, R., 1999. Concomitant and controlled release of dexamethasone and 5-fluorouracil from poly(ortho ester). Int. J. Pharm. 185, 189–198.

Ende, M.T.A., Peppas, N.A., 1997. Transport of ionizable drugs and proteins in crosslinked poly(acrylic acid) and poly(acrylic acid-*co*-2-hydroxyethyl methacrylate) hydrogels.2. Diffusion and release studies. J. Controlled Release 48, 47–56.

Flynn, G.L., Lamb, D.J., 1970. Factors influencing solvolysis of corticosteroid-21-phosphate esters. J. Pharm. Sci. 59, 1433–1438.

Fristrom, B., 1996. A 6-month, randomized, double-masked comparison of latanoprost with timolol in patients with open angle glaucoma or ocular hypertension. Acta Ophthalmol. Scan. 74, 140–144.

Hillman, J.S., 1974. Management of acute glaucoma with pilocarpine-soaked hydrophilic lens. Br. J. Ophthalmol. 58, 674–679.

Hiratani, H., Alvarez-Lorenzo, C., 2004. The nature of backbone monomers determines the performance of imprinted soft contact lenses as timolol drug delivery systems. Biomaterials 25, 1105–1113.

Hiratani, H., Fujiwara, A., Tamiya, Y., Mizutani, Y., Alvarez-Lorenzo, C., 2005. Ocular release of timolol from molecularly imprinted soft contact lenses. Biomaterials 26, 1293–1298.

Li, C.C., Chauhan, A., 2006. Modeling ophthalmic drug delivery by soaked contact lenses. Ind. Eng. Chem. Res. 45, 3718–3734.

Mcnamara, N.A., Polse, K.A., Brand, R.J., Graham, A.D., Chan, J.S., Mckenney, C.D., 1999. Tear mixing under a soft contact lens: effects of lens diameter. Am. J. Ophthalmol. 127, 659–665.

Melby, J.C., 1974. Drug spotlight program: Systemic corticosteroid therapy: Pharmacology and endocrinologic considerations. Ann. Intern. Med. 81, 505–512.

Ogura, Y., 2001. Drug delivery to the posterior segments of the eye. Adv. Drug Deliv. Rev 52, 1–3.

Ramer, R.M., Gasset, A.R., 1974. Ocular penetration of pilocarpine: The effect of hydrophilic soft contact lenses on the ocular penetration of pilocarpine. Ann. Ophthalmol. 6, 1325–1327.

Rosenwald, P.L., 1984. Occular device. US Patent 4,484,922 (27 November).

Ruben, M., Watkins, R., 1975. Pilocarpine dispensation for the soft hydrophilic contact lens. Br. J. Ophthalmol. 59, 455–458.

Schultz, C.L., Nunez, I.M., Silor, D.L., Neil, M.L., 1998. Contact lens containing a leachable absorbed material. US Patent 5,723,131 (03 March).

Schultz, C.L., Mint, J.M., 2002. Drug delivery system for antiglaucomatous medication. US Patent 6,410,045 (25 June).

Schwartz, B., 1966. The response of ocular pressure to corticosteroids. Int. Ophthalmol. Clin. 6, 929–989.

Urban, R.C., Cotlier, E., 1986. Corticosteroid-induced cataracts. Surv. Ophthalmol. 31, 102–110.

Ward, J.H., Peppas, N.A., 2001. Preparation of controlled release systems by free-radical UV polymerizations in the presence of a drug. J. Controlled Release 71, 183–192.

Weijtens, O., Vandersluijs, F.A., Schoemaker, R.C., Lentjes, E.G.W.M., Cohen, A.F., Romijn, F.P.H.T.M., Vanmeurs, J.C., 1997. Peribulbar corticosteroid injection: vitreal and serum concentrations after dexamethasone disodium phosphate injection. Am. J. Ophthalmol. 123, 358–363.

Weijtens, O., Schoemaker, R.C., Cohen, A.F., Romijn, F.P.H.T.M., Lentjes, E.G.W.M., Van Rooij, J., Van Meurs, J.C., 1998. Dexamethasone concentration in vitreous and serum after oral administration. Am. J. Ophthalmol. 125, 673–679.

Weijtens, O., Feron, E.J., Schoemaker, R.C., Cohen, A.F., Lentjes, E.G.W.M., Romijn, F.P.H.T.M., Van Meurs, J.C., 1999. High concentration of dexamethasone in aqueous and vitreous after subconjunctival injection. Am. J. Ophthalmol. 128, 192–197.

Weijtens, O., Schoemaker, R.C., Lentjes, E.G.W.M., Romijn, F.P.H.T.M., Cohen, A.F., Van Meurs, J.C., 2000. Dexamethasone concentration in the subretinal fluid after a subconjunctival injection, a peribulbar injection, or an oral dose. Ophthalmology 107, 1932–1938.

Weijtens, O., Schoemaker, R.C., Romijn, F.P.H.T.M., Cohen, A.F., Lentjes, E.G.W.M., Van Meurs, J.C., 2002. Intraocular penetration and systemic absorption after topical application of dexamethasone disodium phosphate. Ophthalmology 109, 1887–1891.

Wilson, M.C., Shields, M.B., 1989. A comparison of the clinical variations of the iridocorneal endothelial syndrome. Arch. Ophthalmol. 107, 1465–1468.